Characterizing Corneal Mechanical Response Using Ocular Pulse Elastography

Keyton Clayson[a,b], Elias Pavlatos[a], Xueliang Pan[c], Tommy Sandwisch[a], Yanhui Ma[a], Jun Liu[a,b,d]

From the [a]Department of Biomedical Engineering, [b]Biophysics Graduate Program, [c]Department of Biomedical Informatics, and [d] Department of Ophthalmology and Visual Science, The Ohio State University, Columbus, OH 43210

Abstract

In vivo measurement of corneal biomechanics remains an important and challenging goal. We have developed a method, termed ocular pulse elastography (OPE), to evaluate the cornea's biomechanical response to the intrinsic cyclic fluctuation of the intraocular pressure (IOP). In this study, we measured corneal deformation induced by ocular pulses in human donor eyes at different simulated ocular pulse amplitudes (OPA), heart rates (HR), and baseline IOP. Our goal was to evaluate how these physiological variations affect corneal biomechanical responses. Ocular pulses were induced via a programmable syringe pump in ten human donor globes. The baseline IOP, HR, and OPA were varied from the nominal condition (15 mmHg, 72 beats per minute (BPM), 3 mmHg, respectively) to baseline IOP= 10 or 20 mmHg, HR= 45 or 100 BPM, or OPA= 1 or 5 mmHg. The deformation of the central 5.7 mm of the cornea was imaged using a 50 MHz ultrasound system at a frame rate of 128 Hz. Through-thickness axial strains were obtained using a speckle tracking algorithm, and a stiffness measure (termed ocular pulse stiffness index, OPSI) was calculated using the IOP-strain data from five pulse cycles. Our results showed that corneal strains were highly dependent on baseline IOP and OPA (p's<0.05, linear mixed model), but not HR (p's>0.05, linear mixed model). In contrast, the OPSI was not different in the same eye under

different OPA, HR, or baseline IOP (p=0.738, linear mixed models). These results suggest that OPE can reliably measure corneal strains induced by the ocular pulse, and the OPSI may provide a robust and sensitive method for quantifying corneal stiffness in vivo.

1. Introduction

Corneal biomechanical properties are important determinants of the cornea's shape and function. Alterations in corneal stiffness may be early indicators of corneal pathologies including keratoconus or iatrogenic ectasia subsequent to refractive surgery.[1,2] Knowledge of corneal biomechanical properties may also be useful for the clinical management of glaucoma, as corneal stiffness affects the accuracy of IOP measurement[3] and may contribute to glaucoma risk through its impact on the dynamic profile of IOP.[4-6] The ability to measure corneal biomechanics in vivo will help clinicians better understand ocular diseases and identify effective treatment strategies.

Current noninvasive methods for in vivo measurement of corneal biomechanics can be largely divided into two groups: the air puff-based and the imaging-based techniques. The air puff-based techniques, including the Ocular Response Analyzer (ORA)[7] and the CorVis ST,[8] have excellent translational capability;[9] however, parameters derived from these methods are for the whole cornea, limiting their ability to spatially resolve potentially heterogeneous corneal properties implicated in pathologic states. Imaging-based techniques including Brillouin microscopy,[10,11] optical coherence tomography (OCT),[12,13] and high-frequency ultrasound[14,15] provides excellent spatial resolution, but are either insensitive to changes in IOP or require large external loading sources to induce a detectable mechanical response.

Our laboratory is among the first to propose a method that utilizes the cornea's intrinsic pulsation as the source of mechanical loading, thus eliminating the need for external excitation. We have previously reported high accuracy and repeatability of a technique, called ocular pulse

elastography (OPE), which utilizes high-frequency ultrasound speckle tracking to measure corneal strains in response to the ocular pulse through the full thickness of the cornea.[17] This technique utilizes densely sampled ultrasound radiofrequency data to achieve a displacement sensitivity and accuracy much higher than the spatial resolution of the imaging system. Using similar correlation-based ultrasound speckle tracking techniques, others have reported achieving an axial displacement accuracy of 0.63-0.73 μm at a frequency of 7.5 MHz.[18] Our previous studies have demonstrated an accuracy of less than 10% error for a 0.5 μm axial displacement, and the same level of accuracy for 0.01% axial strain and 0.025% lateral strain.[17]

In this study, we applied the OPE technique to measure corneal strains in human donor eyes, and evaluated the influence of several physiological variables, including simulated ocular pulse amplitude (OPA), heart rate (HR), and baseline IOP, on corneal strains. Since strain is influenced by both intrinsic material properties and loading conditions (i.e. IOP characteristics), we propose a new parameter derived from the ocular pulse measurement (called the ocular pulse stiffness index, OPSI) to capture the intrinsic tissue response.[17] In this study, the OPSI was calculated and compared under different simulated OPA, HR, and baseline IOP conditions to evaluate whether it can be used as an IOP-independent stiffness measure.

2. Methods

2.1. Human donor globe preparation

Human donor globes with no known history of ocular trauma, ocular surgery, or corneal diseases were obtained from the Lions Eye Bank of West Central Ohio (Dayton, OH), transported at 4^{o} C in a sealed moist container, and tested within 48 hours postmortem. To reverse the effects of postmortem corneal swelling, globes were pretreated in 3.5% poloxamer-188 solution in 0.9%

saline (Kolliphor® 188, Sigma Aldrich, St. Louis, MO; hereafter referred to as P188) at 4° C,[20] with IOP being maintained near 15 mmHg via a column and the anterior chamber being perfused with the same P188 solution, for at least 18 hours until corneal thickness stabilized. The globes remained immersed in this 3.5% P188 solution to maintain corneal hydration status during all testing described below.

The experimental setup is presented in Fig. 1A. Globes were secured to a custom-built holder using two 20G spinal needles inserted at the equator of the eye (Fig. 1B). A 20G hypodermic needle attached to a fluid column and programmable syringe pump (PhD Ultra, Harvard Apparatus, Boston, MA) was inserted into the anterior chamber through the limbus along the superior-inferior axis and was used to control baseline IOP and ocular pulse. Another 20G needle attached to a pressure sensor (P75 venous pressure transducer, Harvard Apparatus) was inserted along the same axis and was used to monitor IOP during experimentation (Fig. 1B).

2.2. OPE testing with various IOP parameters

Prior to testing, all globes were preconditioned with 25 pressure cycles from 5 to 30 mmHg and stabilized at a baseline IOP of 15 mmHg at room temperature for at least 30 minutes. Each OPE test consisted of 25 ocular pulse cycles at a specified simulated ocular pulse amplitude (OPA), heart rate (HR), and baseline IOP (Fig. 1C). During the last 5 cycles of each test, radiofrequency data of the B-mode images of the central 5.7 mm cornea were acquired by a 50 MHz ultrasound probe (MS700, VisualSonics, Toronto) along the nasal-temporal meridian at a frame rate of 128 frames per second (Fig. 1D).

The globes first underwent a test under the nominal conditions (the nom group), which were defined as a baseline IOP of 15 mmHg, a HR of 72 beats per minute (BPM), and an OPA of

3 mmHg. The globes then underwent a series of tests where one parameter at a time was varied from the nominal condition: baseline IOP of 10 or 20 mmHg (the base group), HR of 45 or 100 BPM (the HR group), or OPA of 1 or 5 mmHg (the OPA group), with a nominal condition test repeated after each variation group (Fig. 2). Globes were equilibrated for 15 minutes after a change in baseline IOP, while tests performed at the same baseline IOP were performed immediately after the previous test. Another nominal condition test was repeated at the end of the study (nom4, Fig. 2). Based on our previous study, OPE tests are highly repeatable in human donor eyes with an intraclass correlation of 0.98.[17] The repeated nominal condition tests at different time points in the present study were used to identify eyes with significant alterations or consistent trends of alteration in their nominal response during the experimentation period. Eyes whose nominal response had significant changes during the experimentation were excluded from further analysis.

2.3. Data Analysis

The general process of the ultrasound speckle tracking method has been described previously.[17,21] Briefly, a region of interest is defined in the first image of each cycle (i.e. the reference image). Within this region, overlapping (75%) kernels 51 x 41 pixels (axial x lateral), or approximately 75 μm x 780 μm, in size are defined. A cross-correlation based algorithm is used to find the new location of each kernel in the next consecutive image (i.e. the deformed image) within a predefined search window, where the highest correlation coefficient is used as the new location of the kernel. Spline interpolation of the correlation coefficients is then applied to find the maximum correlation coefficient at sub-pixel resolution, thus achieving displacement identification at the sub-pixel level. Axial strain along each column of kernels is then calculated using a robust fit multilinear regression based on the displacements of the kernels from anterior to

posterior cornea (*regress* function in MATLAB, r2014a, The Mathworks, Inc., Natick, MA). Strain maps are generated to visualize the spatial distribution of strain interpolated at each pixel.

The axial strain averaged over all kernels within the region of interest at peak pressure was further analyzed to derive a biomechanical index that is independent of IOP, as described previously.[17] The strategy is to use the OPE data to reproduce the cornea's inflation response based on the characteristic nonlinear relationship between IOP and the resultant strain. Based on our previous experimental data in human eyes, the corneal inflation strain response can be captured by the following equation:

$$Strain = \frac{-1}{OPSI} \cdot ln(IOP/IOP_0) \quad (1)$$

where IOP_0 is the reference pressure at which zero strain is assumed, and OPSI stands for "ocular pulse stiffness index," which is a fitting parameter. The OPSI reflects the overall stiffness of the cornea, as shown in Fig. 3A: a larger OPSI value corresponds to a stiffer corneal response (i.e. smaller strain) to increases in IOP. It is noted that this value captures the entire inflation response rather than at any specific IOP level, and in this sense OPSI is IOP-independent.

At a given IOP, the slope of the inflation curve (denoted as *k*) can be obtained by taking the derivative of strain with respect to IOP. This is illustrated in Figure 3A, where the grey line shows the slope of the inflation curve at a certain IOP. By taking the derivative of Equation (1) with respect to IOP, we obtain the following equation:

$$k = \frac{-1}{OPSI \cdot IOP} \quad (2)$$

The slope *k* at IOP = (baseline IOP + ½ OPA) can be estimated from OPE strains obtained from multiple testing cycles (Fig. 3B) by dividing the average peak strain by the ocular pulse amplitude (OPA). The *k* value was then used to calculate OPSI using Equation (2).

2.4. Statistical Analysis

All data analysis results were conducted using SAS 9.4. Axial strains at peak pressure and OPSI values were summarized using mean and standard deviation. Axial strains and OPSI values for each condition were compared using linear mixed models with repeated measures. The repeatability of the OPSI from the four nominal conditions was evaluated using the intraclass correlation (ICC) and the signal-to-noise ratio (SNR) as described in our previous paper.[17]

3. Results

Fourteen globes were tested in this study and four were excluded from analysis due to significant alterations in nominal conditions. The alternation in nominal condition response was likely due to unstable infusion response in these eyes as suggested by significantly altered infusion parameters during experimentation, indicating changes in either the eye or the infusion tubing setup (e.g., unstable flow rate or pressure response).

Ocular pulse induced corneal strains were calculated in each donor eye under each test condition. Representative maps of axial strains under different baseline IOP, OPA, and heart rate are shown in Figure 4 to illustrate the trend of how corneal strains changed under different condition. Overall, the simulated physiological variables (baseline IOP, OPA, and heart rate) had a significant influence on corneal strains ($p<0.001$, linear mixed models). Specifically, changes in baseline IOP from 15 to 10 mmHg resulted in a significant increase in corneal strain (-0.070%±0.021% vs. -0.115%±0.066%, $p=0.030$), while changes in baseline IOP from 15 to 20 mmHg resulted in a significant decrease in corneal strain (-0.070%±0.021% vs. -0.050%±0.015%, $p<0.001$). Changes in OPA from 3 to 1 mmHg resulted in a significant decrease in corneal strain (-0.070%±0.021% vs. -0.027%±0.010%, $p<0.001$), while changes in OPA from 3 to 5 mmHg

resulted in a significant increase in corneal strain (-0.070%±0.021% vs. -0.105%±0.039%, p=0.001). Changes from 72 to 45 or 100 BPM did not result in significant changes in corneal strains (p's>0.05). The strains under the four nominal conditions measured throughout the experimental period were not significantly different (nom1= -0.067%±0.025%, nom2= -0.071%±0.021%, nom3= -0.072%± 0.024%, and nom4= -0.071%±0.023%, all p's>0.05). The largest corneal strains were obtained at a baseline IOP of 10 mmHg (-0.115%±0.066%), while the smallest were obtained at an OPA of 1 mmHg (-0.027%±0.010%).

The average strain and OPSI values obtained from OPE measurements in the 10 tested human donor corneas are shown in Figure 5. Despite significant differences in strains, the OPSI in human eyes was not different from the nominal conditions when measured under different baseline IOP, OPA, or heart rate (OPA1= 290±110, OPA5= 313±130, base10= 315±164, base20= 323±137, HR45= 299±122, HR100= 316±140, nom1= 315±150, nom2= 295±100, nom3= 310±125, nom4= 300±123, linear mixed models, p=0.738). Additional analyses were performed to compare OPSI between the two extremes of each variable (i.e. comparing OPA1 and OPA5, base10 and base20, and HR45 and HR100). The difference between OPA 1 and OPA5 was the largest; nonetheless, the difference (i.e. 23) was not significant (p=0.09) and smaller than the pooled intrasubject standard deviation (i.e. 28.3) over the four nominal conditions in the ten eyes.

The ICC for the four nominal conditions was 0.979, suggesting the OPSI measures were highly consistent in the repeated measurements. Also, the two SNR values, evaluated in two different ways (first, the ratio of the variance between samples and the variance within samples; second, the ratio of the mean OPSI and the pooled standard deviation), were 18.6 and 10.3, respectively, which were both above the necessary minimum value of 5 established by the Rose criterion [22]. A plot of the OPSI value versus the average axial strain in each individual donor eye

averaged over the 4 repeated nominal conditions is shown in Figure 6 to illustrate the range of the OPSI and axial strains across different donors.

4. Discussion and Conclusions

In this study, we utilized a high-frequency ultrasound speckle tracking technique, ocular pulse elastography (OPE), to measure the cornea's response to the cyclic ocular pulse under varying physiological conditions. Our results showed that the OPE technique can detect changes in corneal strains under different conditions, while the derived stiffness measure, the OPSI, was not influenced by physiological variations. These results indicate that the OPE technique combined with the OPSI parameter may provide a sensitive and robust method for characterizing corneal stiffness.

The ocular pulse induces a thinning of the cornea in the through-thickness direction, indicated by the negative axial strains throughout the corneal thickness (Fig. 4). This thinning primarily results from the stretch of the cornea during an increase in IOP and is dependent on both the biomechanical properties of the cornea and the IOP characteristics discussed below. The level of thinning (i.e., the magnitude of the axial strains) was significantly different when the baseline IOP was changed from 15 to 10 or 20 mmHg while the OPA and HR were kept the same. Differences in corneal strains at different baseline IOP can be explained by the known nonlinear mechanical behavior of the cornea[4,23] which manifests as a more compliant response at a lower IOP and a stiffer response at a higher IOP. The axial strain was also significantly different when the OPA was changed from 3 to 1 or 5 mmHg while the baseline IOP and HR were kept the same. Although it is expected that a larger load would generate a larger deformation, this result demonstrates the sensitivity of the OPE approach, at it consistently and robustly differentiates the differences in corneal responses within the small physiological range of OPA.

As expected, the strains at low OPA (i.e. 1 mmHg) were small (average -0.027%±0.010%, range -0.014% to -0.043%), approaching the detection limit of our ultrasound technique in some eyes (less than 10% error for axial strains equal to or higher than 0.01%).[17] Literature reports of the OPA range in living patients as measured by dynamic contour tonometry (DCT) indicate the OPA magnitude is higher than 1 mmHg in most eyes.[29-31] Clinically, we anticipate that it is more important to accurately detect and quantify larger strains which indicate weaker corneas or regional weakening associated with ectatic risk.

An important goal in corneal biomechanical characterization is to identify parameters that are primarily dependent on the cornea itself, with less influence from other physiological variables such as IOP at the time of measurement. This is the motivation for deriving the OPSI from the measured ocular pulse strains, as the strain magnitudes are dependent on the loading parameters. As described earlier, the OPSI is calculated from the slope of strain at a given IOP (see Equation 2), and this parameter reflects the overall stiffness of the cornea's inflation response (Fig. 3A). Based on our experimental data, the OPSI had minimal dependence on the testing conditions (Fig. 5) and was inversely related to axial strain when testing conditions were held constant (Fig. 6) in human donor eyes, suggesting that it can be used to represent the mechanical stiffness of the cornea independent of the loading parameters. It is noted that to calculate OPSI, the characteristics of the ocular pulse need to be known for the measured eye. This can be achieved in vivo using an IOP measurement device that reports both systolic and diastolic IOP, such as the Pascal Dynamic Contour Tonometer.[33]

We envision that a major challenge in translating this technique to in vivo use is to maintain the displacement and strain accuracy in the presence of additional motion noise, including both biological (e.g. eye motion, head motion, etc.) and environmental (e.g. building vibrations, etc.)

sources. In our ongoing work to achieve such a goal, we found that experimentation on ex vivo globes was helpful in providing several noise-reduced datasets needed to interpret the in vivo measurements in the presence of noise. In addition, we have demonstrated that using a scanning frame rate over 100 frames per second, a strategy frequently adopted in the field of myocardium ultrasound elastography,[34] we can achieve successful tracking in vivo with correlation coefficients over 0.9 in the presence of extraneous motion (unpublished results).

There are a few limitations in the present study. First, corneal hydration has been shown to significantly impact mechanical response.[35-37] In this study, we used immersion in P188 solution to control corneal hydration before and during OPE tests.[20] Although the tissue hydration levels might not be the same as the in vivo condition, stable hydration during experimentation was indicated by the repeatable outcomes of tests under nominal conditions performed throughout the experiments. Second, the current study has focused on evaluating axial strain through the corneal thickness. The through-thickness thinning during pressure increase are influenced by the in-plane material properties. Our previous studies have shown a strong correlation between radial and tangential strains in sclera[38] and cornea[15, 39] at all pressure levels tested during inflation. Future work will further improve the lateral analysis in OPE tests to better characterize the in-plane response and the full 2D strain profile of the cornea. Finally, the ex vivo experimentation setup is limited in maintaining a stable response in the tested eyes due to the difficulty in controlling infusion and flow stability during lengthy experimentation (>3 hours at room temperature) with many infusion/withdrawal cycles, which may have resulted in the lower than typical yield of usable data. Further in vivo studies in animal models may be needed to fully characterize the influence of physiological variables on OPE measured strains and OPSI.

In summary, we have developed and validated a non-invasive OPE technique to measure the through-thickness strains of the human cornea in response to the ocular pulse. This approach takes advantage of the naturally occurring ocular pulse and utilizes high frequency and high frame rate ultrasound speckle tracking to measure corneal strains during cyclic IOP changes. The approach also utilizes a biomechanical parameter, OPSI, to quantify corneal stiffness independent of physiological parameters including OPA, IOP, and heart rate. These unique qualities may help translate this technique to a clinical tool for in vivo imaging of corneal biomechanics to improve diagnosis and therapeutic planning of ocular diseases.

References

1. Piñero DP, Alcón N. In vivo characterization of corneal biomechanics. J Cataract Refract Surg. 2014;40:870.

2. Ruberti JW, Sinha Roy A, Roberts CJ. Corneal Biomechanics and Biomaterials. Annu Rev Biomed Eng. 2011;13:269-295.

3. Liu J, Roberts CJ. Influence of corneal biomechanical properties on intraocular pressure measurement. J Cataract Refract Surg. 2005;31:146-155.

4. Clayson K, Pan X, Pavlatos E, et al. Corneoscleral stiffening increases IOP spike magnitudes during rapid microvolumetric change in the eye. Exp Eye Res. 2017;165:29-34.

5. He X, Liu J. A Quantitative Ultrasonic Spectroscopy Method for Noninvasive Determination of Corneal Biomechanical Properties. Invest Ophthalmol Vis Sci. 2009;50:5148.

6. Markert JE, Jasien JV, Turner DC, Huisingh C, Girkin CA, Downs JC. IOP, IOP Transient Impulse, Ocular Perfusion Pressure, and Mean Arterial Pressure Relationships in Nonhuman Primates Instrumented With Telemetry. Invest Ophthalmol Vis Sci. 2018;59:4496.

7. Luce DA. Determining in vivo biomechanical properties of the cornea with an ocular response analyzer. J Cataract Refract Surg. 2005;31:156-162.

8. Ambrósio Jr R, Ramos I, Luz A, et al. Dynamic ultra high speed Scheimpflug imaging for assessing corneal biomechanical properties. Rev Bras Oftalmol. 2013;72:99-102.

9. Vinciguerra R, Ambrósio R, Elsheikh A, et al. Detection of Keratoconus With a New Biomechanical Index. J Refract Surg. 2016;32:803-810.

10. Scarcelli G, Besner S, Pineda R, Yun SH. Biomechanical characterization of keratoconus corneas ex vivo with Brillouin microscopy. Invest Ophthalmol Vis Sci. 2014;55:4490-4495.

11. Scarcelli G, Besner S, Pineda R, Kalout P, Yun SH. In Vivo Biomechanical Mapping of Normal and Keratoconus Corneas. JAMA Ophthalmol. 2015;133:480-482.

12. Ford MR, Roy AS, Rollins AM, Dupps WJ. Serial biomechanical comparison of edematous, normal, and collagen crosslinked human donor corneas using optical coherence elastography. J Cataract Refract Surg. 2014;40:1041-1047.

13. Han Z, Li J, Singh M, et al. Optical coherence elastography assessment of corneal viscoelasticity with a modified Rayleigh-Lamb wave model. J Mech Behav Biomed Mater. 2017;66:87-94.

14. Hollman K, Shtein RM, Tripathy S, Kim K. Using an Ultrasound Elasticity Microscope to Map Three-Dimensional Strain in a Porcine Cornea. Ultrasound Med Biol. 2013;39:1451-1459.

15. Palko JR, Tang J, Cruz Perez B, Pan X, Liu J. Spatially heterogeneous corneal mechanical responses before and after riboflavin–ultraviolet-A crosslinking. J Cataract Refract Surg. 2014;40:1021-1031.

16. Hollman K, Emelianov S, Neiss J, et al. Strain Imaging of Corneal Tissue With an Ultrasound Elasticity Microscope. Cornea. 2002;21:68-73.

17. Pavlatos E, Chen H, Clayson K, Pan X, Liu J. Imaging Corneal Biomechanical Responses to Ocular Pulse Using High-Frequency Ultrasound. IEEE Trans Med Imaging. 2018;37:663-670.

18. Hansen HHG, Lopata RGP, Idzenga T, de Korte CL. Full 2D displacement vector and strain tensor estimation for superficial tissue using beam-steered ultrasound imaging. Phys Med Biol. 2010;55:3201-3218.

19. Akyildiz AC, Hansen HH, Nieuwstadt HA, et al. A Framework for Local Mechanical Characterization of Atherosclerotic Plaques: Combination of Ultrasound Displacement Imaging and Inverse Finite Element Analysis. Ann Biomed Eng. 2016;44:968-979.

20. Zhao M, Thuret G, Piselli S, et al. Use of Poloxamers for Deswelling of Organ-Cultured Corneas. Invest Ophthalmol Vis Sci
. 2008;49:550-559.

21. Tang J, Liu J. Ultrasonic measurement of scleral cross-sectional strains during elevations of intraocular pressure: method validation and initial results in posterior porcine sclera. J Biomech Eng. 2012;134:091007.

22. Bushburg JT. The Essential Physics of Medical Imaging. 2nd ed. Philadelphia, PA: Williams & Wilkins; 2006:p. 280.

23. Woo SL, Kobayashi AS, Schlegel WA, Lawrence C. Nonlinear material properties of intact cornea and sclera. Exp Eye Res. 1972;14:29-39.

24. Boyce BL, Jones RE, Nguyen TD, Grazier JM. Stress-controlled viscoelastic tensile response of bovine cornea. J Biomech. 2006;40:2367-2376.

25. Elsheikh A, Wang D, Rama P, Campanelli M, Garway-Heath D. Experimental Assessment of Human Corneal Hysteresis. Curr Eye Res. 2008;33:205-213.

26. Elsheikh A, Anderson K. Comparative study of corneal strip extensometry and inflation tests. J R Soc Interface. 2005;2:177-185.

27. Elsheikh A, Wang D, Pye D. Determination of the modulus of elasticity of the human cornea. J Refract Surg. 2007;23:808-818.

28. Kaplan D, Bettelheim FA. Dynamic Rheotopical Behavior of Isolated Bovine Cornea. Biophys J. 1972;12:1630-1641.

29. Fogagnolo P, Figus M, Frezzotti P, et al. Test-retest variability of intraocular pressure and ocular pulse amplitude for dynamic contour tonometry: a multicentre study. Br J Ophthalmol. 2010;94:419-423.

30. Knecht PB, Menghini M, Bachmann LM, Baumgartner RW, Landau K. The Ocular Pulse Amplitude as a Noninvasive Parameter for Carotid Artery Stenosis Screening: A Test Accuracy Study. Ophthalmol. 2012;119:1244-1249.

31. Kaufmann C, Bachmann LM, Robert YC, Thiel MA. Ocular Pulse Amplitude in Healthy Subjects as Measured by Dynamic Contour Tonometry. Arch Ophthalmol. 2006;124:1104-1108.

32. Punjabi OS, Ho HV, Kniestedt C, Bostrom AG, Stamper RL, Lin SC. Intraocular Pressure and Ocular Pulse Amplitude Comparisons in Different Types of Glaucoma Using Dynamic Contour Tonometry. Curr Eye Res. 2006;31:851-862.

33. Kanngiesser H, Kniestedt C, Robert Y. Dynamic Contour Tonometry: Presentation of a New Tonometer. J Glaucoma. 2005;14:344-350.

34. Lee W, Provost J, Fujikura K, Wang J, Konofagou EE. In vivo study of myocardial elastography under graded ischemia conditions. Phys Med Biol. 2011;56:1155.

35. Clayson K, Pavlatos E, Ma Y, Liu J. 3D Characterization of corneal deformation using ultrasound speckle tracking. J Innov Opt Health Sci. 2017;10:8.

36. Dias J, Ziebarth N. Impact of Hydration Media on Ex Vivo Corneal Elasticity Measurements. Eye Contact Lens. 2015;41:281-286.

37. Hatami-Marbini H, Etebu E. Hydration dependent biomechanical properties of the corneal stroma. Exp Eye Res. 2013;116:47-54.

38. Morris HJ, Tang J, Cruz Perez B, et al. Correlation Between Biomechanical Responses of Posterior Sclera and IOP Elevations During Micro Intraocular Volume Change. Invest Ophthalmol Vis Sci. 2013;54:7215.

39. Palko JR, Morris HJ, Pan X, et al. Influence of Age on Ocular Biomechanical Properties in a Canine Glaucoma Model with ADAMTS10 Mutation. PLoS One. 2016;11:e0156466.

Figure 1

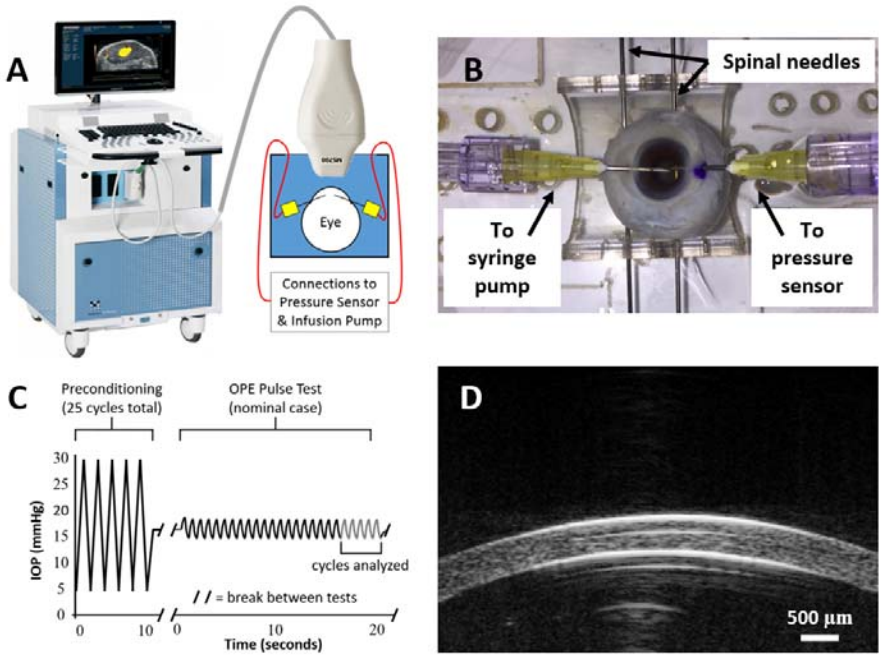

Figure 1: **A** Illustration of the experimental setup, with globe fully immersed during experiments. **B** Globe mounted on a holder using spinal needles, with pressure control and monitoring. **C** IOP loading protocol for OPE experiments, with pulse parameters modified for each variation. **D** Representative high-frequency B-mode ultrasound image of a human donor cornea after deswelling in P188.

Figure 2

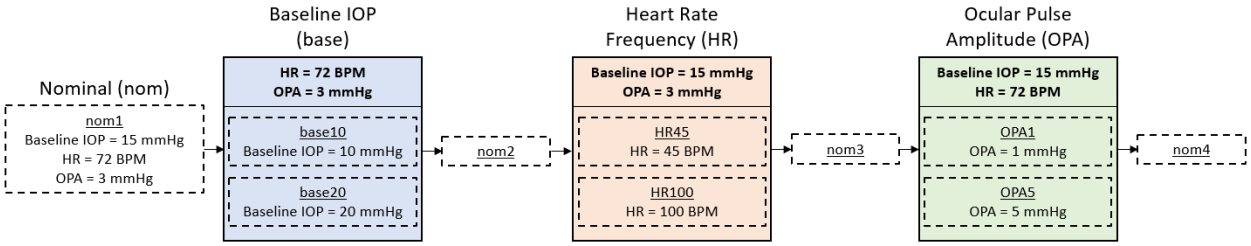

Figure 2: Flow chart of experimental conditions for OPE tests in human donor eyes. OPA = ocular pulse amplitude, HR = heart rate, BPM = beats per minute.

Figure 3

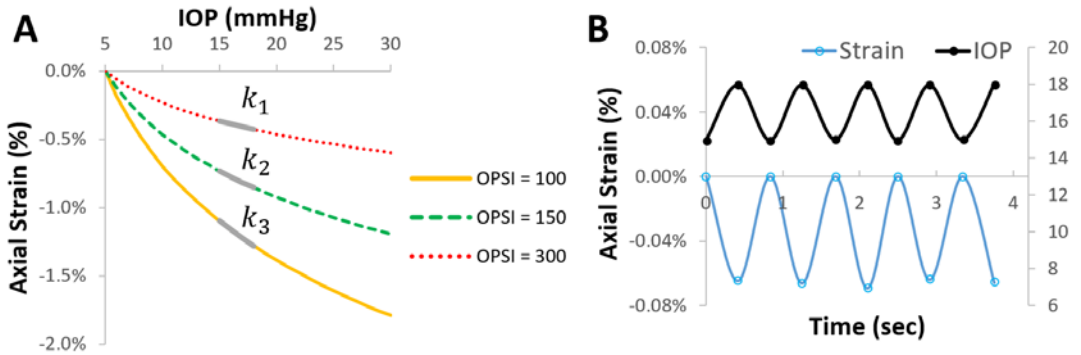

Figure 3: **A** Inflation curves illustrating the nonlinear relationship between corneal strain and IOP. A higher ocular pulse stiffness index (OPSI) value translates to a stiffer corneal response to elevated IOP. *k* is the slope of the inflation curve at a given IOP. **B** Corneal axial strain (open circles with line) and IOP (black dots) from multiple cycles of OPE testing in a human donor eye.

Figure 4

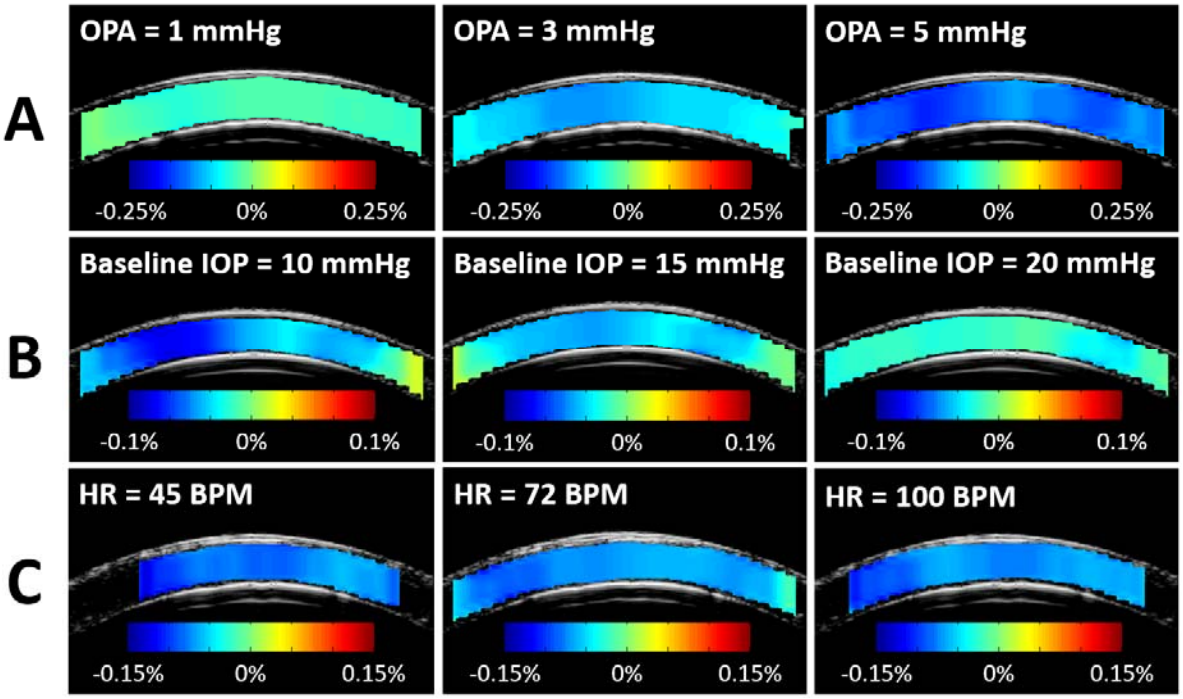

Figure 4: Corneal strain maps in three representative human eyes. **(A)** Corneal strain maps in a donor eye as OPA changed from 1 to 5 mmHg. Baseline IOP and HR were kept at nominal values. **(B)** Corneal strain maps in a donor eye as baseline IOP changed from 10 to 20 mmHg. OPA and HR were kept at nominal values. **(C)** Corneal strain maps in a donor eye as HR changed from 45 to 100 BPM. Baseline IOP and OPA were kept at nominal values.

Figure 5

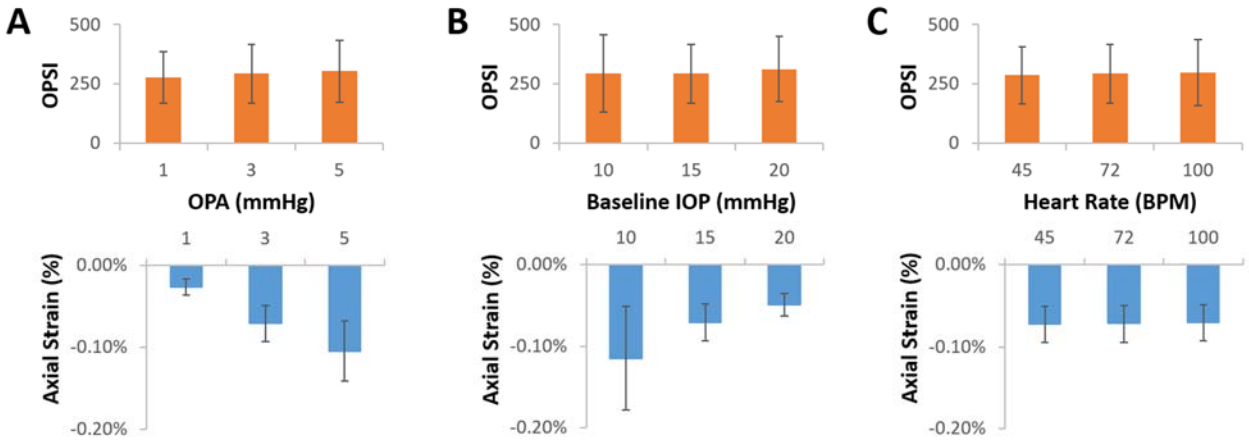

Figure 5: Comparison of OPSI and corneal axial strains by variations in OPA (**A**), baseline IOP (**B**), and heart rate (**C**) in human corneas. Corneal strains were influenced by OPA and baseline IOP, but not heart rate. In contrast, OPSI values were not significantly different for different OPA, baseline IOP, and HR (p=0.738, linear mixed models). BPM= beats per minute.

Figure 6

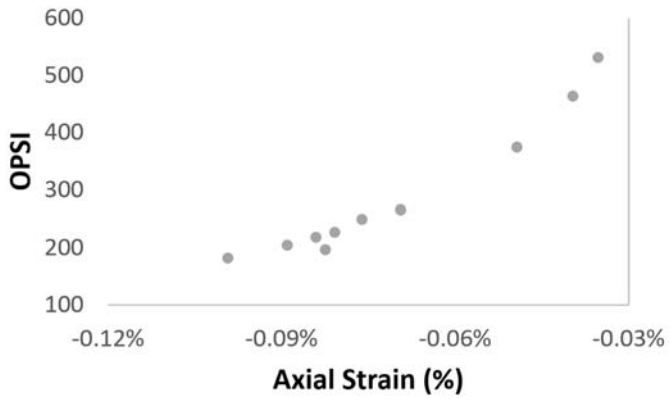

Figure 6: OPSI value versus average axial strain under nominal conditions in each tested donor eye.